J|A|C|S
ARTICLES
Published on Web 10/03/2002

# Formation of Adenine−N3/Guanine−N7 Cross-Link in the Reaction of trans-Oriented Platinum Substrates with Dinucleotides

Yangzhong Liu,† Jo Vinje,† Concetta Pacifico,‡ Giovanni Natile,‡ and Einar Sletten*,†

*Contribution from the Department of Chemistry, University of Bergen, Allegt. 41, N-5007 Bergen, Norway, and Dipartimento Farmaco-Chimico, University of Bari, via E. Orabona 4, I-70125, Bari, Italy*

Received June 11, 2002

***Abstract:*** The reactions of the anticancer complex *trans*-[$PtCl_2$\{(*E*)-HN═C(OMe)Me\}$_2$] (*trans-EE*) with a series of ribo and deoxyribodinucleotides have been studied by HPLC and 2D [$^1$H, $^{15}$N] HMQC NMR spectroscopy and compared with those of the inactive trans isomer of cisplatin, *trans*-[$PtCl_2(NH_3)_2$] (*trans*-DDP). Reactions of *trans-EE* with r(ApG) and d(ApG) take place through solvolysis of the starting substrate and subsequent formation of trans G−N7/monochloro and G−N7/monoaqua adducts. Slowly, the monofunctional adducts evolve to a bifunctional adduct forming an unprecedented and unexpected A−N3/G−N7 platinum cross-link spanning two trans positions. For stereochemical reasons, trans platinum complexes cannot form N7/N7 cross-links between adjacent purines in di- or polynucleotides. For the reverse sequence r(GpA), no chelate structure was formed even after a two-week reaction. The reaction of *trans*-DDP with r(ApG) produces many more products than the analogous reaction with *trans-EE*. One of these products was identified as the A−N3/G−N7 trans-chelate.

## Introduction

The well-known anticancer drug *cis*-diamminedichloroplatinum(II) (*cis*-DDP) can form a variety of covalent DNA adducts. Although the structure/activity relationship underlining the high efficacy of *cis*-DDP in the treatment of cancers is not fully understood, it is generally believed that the cytotoxic properties are a consequence of its bifunctional binding to DNA.[1] In the major adduct, *cis*-DDP forms 1,2-cross-links between adjacent purines in d(GpG) or d(ApG) sequences. These lesions result in a bending of the helical axis of DNA in the range 25−50° in the direction of the major groove.[2−5] The clinically ineffective *trans*-DDP isomer cannot form these types of 1,2-N7,N7 adducts. However, in the reaction between *trans*-DDP and single-stranded oligonucleotides containing the triplet GNG (N being a nucleotide residue), (G1, G3)-intrastrand cross-links are formed.[6] These intrastrand cross-links are stable as long as the oligonucleotides are single-stranded. After annealing with the complementary strand, the 1,3-intrastrand chelate isomerizes to form an interstrand DNA adduct.[7]

Recently, it has been shown that several analogues of *trans*-DDP exhibit antitumor properties.[8−11] Early examples of in vivo active *trans*-Pt(II) complexes were the *trans*-[$PtCl_2(NH_3)$(thiazole)] and the *trans*-[$PtCl_2$(iminoether)$_2$] species.[9−11] Of particular interest is *trans*-[$PtCl_2$\{(*E*)-HN═C(OMe)Me\}$_2$] (*trans-EE*) which has shown an activity comparable to that of *cis*-DDP in the P338 leukemia system and exerts antitumor effects on Lewis lung carcinoma.[12] The *trans-EE*/DNA binding mode in cell-free medium has been investigated by several biophysical methods. The major DNA lesion formed by the iminoether compound appears to be a monofunctional Pt-binding to the N7 nitrogen of a purine base.[13] Recently we have published a structural analysis of a *trans-EE* platinated duplex formed by platination at G−N7 of the single-strand 5′-d(CCTCG*CTCTC) and subsequently hybridization with its complement 5′-d(GAGAGCGAGG).[14] Interestingly, *trans-EE* platination was found to induce a bending of the helix axis toward the minor

* Address correspondence to this author. E-mail: einar.sletten@kj.uib.no.
† University of Bergen.
‡ University of Bari.

(1) *Cisplatin. Chemistry and Biochemistry of a Leading Anticancer Drug*, Lippert, B., Ed.; Wiley-VCH: Zurich, 1999.
(2) Takahara, P. M.; Rosenzweig, A. C.; Frederick, C. A.; Lippard, S. J. *Nature* **1995**, *377*, 649−652.
(3) Takahara, P. M.; Frederick, C. A.; Lippard, S. J. *J. Am. Chem. Soc.* **1996**, *118*, 12309.
(4) Yang, D. Z.; van Boom, S. S. G. E.; Reedijk, J.; van Boom, J. H.; Wang, A. H. J. *Biochemistry* **1995**, *34*, 12912−12920.
(5) Gelasco, A.; Lippard, S. J. *Biochemistry* **1998**, *37*, 9230−9239.
(6) Comess, K. M.; Costello, C. E.; Lippard, S. J. *Biochemistry* **1990**, *29*, 2102−2110.
(7) Malinge, J. M.; Leng, M. In *Cisplatin. Chemistry and Biochemistry of a Leading Anticancer Drug*; Lippert, B., Ed.; Wiley-VCH: Zurich, 1999; pp 159−180.
(8) Natile, G.; Coluccia, M. *Coord. Chem. Rev.* **2001**, *216*, 383−410.
(9) Coluccia, M.; Nassi, A.; Loseto, F.; Boccarelli, A.; Mariggiò, M. A.; Giordano, D.; Intini, F. P.; Caputo, P.; Natile, G. *J. Med. Chem.* **1993**, *36*, 510−512.
(10) Farrell, N. In *Metal Ions in Biological Systems*; Sigel, A., Sigel, H., Eds.; Marcel Dekker: New York, 1996; Vol. 32, pp 603−639.
(11) Kelland, L. R.; Barnard, C. F. J.; Evans, I. G.; Murrer, B. A.; Theobald, B. R. C.; Wyer, S. B.; Goddard, P. M.; Jones, M.; Valenti, M.; Bryant, A.; Rogers, P. M.; Harrap, K. R. *J. Med. Chem.* **1995**, *38*, 3016−3024.
(12) Coluccia, M.; Fanizzi, F. P.; Giannini, G.; Giordano, D.; Intini, F. P.; Lacidogna, G.; Loseto, F.; Mariggiò, M. A.; Nassi, A.; Natile, G. *Anticancer Res.* **1991**, *11*, 281−287.
(13) Zaludova, R.; Zakovska, A.; Kasparkova, J.; Balcarova, Z.; Vrana, O.; Coluccia, M.; Natile, G.; Brabec, V. *Mol. Pharmacol.* **1997**, *52*, 354−361.
(14) Andersen, B.; Margiotta, N.; Coluccia, M.; Natile, G.; Sletten, E.; *Metal-Based Drugs* **2000**, *7*, 23−32.


**10.1021/ja027251n CCC: $22.00** 

groove by 45°. The magnitude of this bending angle is comparable to that observed in 1,2-bifunctional adducts of cisplatin although in the latter case the bending is directed toward the major groove.

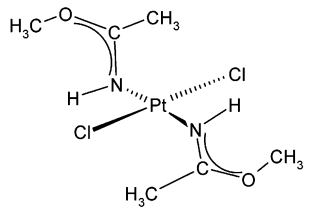

*Trans-EE*

It has been postulated that since *trans*-DDP is more reactive than the cis isomer, undesired side reactions occurring on its way to the pharmacological target are likely to contribute, at least in part, to the lack of anticancer activity.[15] Sterically demanding ligands, like iminoethers in *trans-EE*, could in principle reduce the axial accessibility of the Pt center and slow the hydrolysis reaction and the subsequent substitution of the aqua ligand by biologically relevant substrates. We have recently shown that the reaction between *trans-EE* and GMP proceeds at a significantly lower rate than the corresponding reaction with *trans*-DDP, especially with respect to the formation of bifunctional adducts.[16] In this report, we have extended the investigation to a series of dinucleotides to further explore the stereochemical aspects of these reactions.

One highly unexpected feature soon recognized in the reaction between *trans-EE* and r(ApG) was the formation of a Pt-[A(*N3*),G(*N7*)] cross-link spanning two trans positions.[17] Although this bifunctional adduct was formed at a relatively slow rate by rearrangement of the monofunctional G(*N7*) adduct M1 ($t_{1/2}$ =101 h), nevertheless, the Pt-[A(*N3*),G(*N7*)] adduct could be of biological relevance since A−N3 is readily exposed to platinum in the minor groove. The involvement of the N3 atom of adenine as an alkylation site and in the cleavage reaction of hammerhead ribozyme has recently been demonstrated.[18,19]

*trans-DDP* has generally been considered unable to form 1,2-intrastrand d(GpG) or d(ApG) adducts as a result of the trans disposition of the leaving groups,[15,20] and this inability could be responsible for lack of antitumor activity. In this paper, we wish to address three different questions: (i) Does the A−N3/G−N7 chelate formation occur with both ApG and GpA sequences? (ii) Does it involve both ribo and deoxyribo compounds? (iii) Can this very unusual trans-chelate adduct be formed with *trans*-DDP as well?

## Experimental Section

**Materials and Sample Preparation.** The $^{15}$N labeled *trans-EE* complex was synthesized according to a literature procedure.[21] r(ApG) was purchased from Sigma and used without further purification. d(ApG) and d(GpA) were purchased from DNA Technology A/S (Denmark) and purified by HPLC. Deuterium oxide was purchased from Flurochem Limited Company. The reactions between *trans-EE* and the nucleotides were carried out at 298 K by addition of a stoichiometric amount of the complex to a 1 mM solution of the nucleotide in the dark. Samples were collected for HPLC detection at various time intervals as described previously.[22] The platinated nucleotides were purified by a Waters 626 HPLC instrument using Millenium 32 software. A reverse phase Waters Symmetry C8 column was used with gradient eluant (0−50% methanol) in 50 mM $NaClO_4$ at a flow rate of 0.8 mL/min. The samples for the kinetic experiments were run at an initial pH of 4.5, separated by HPLC, lyophilized, and dissolved into 0.5 mL $D_2O$ or $H_2O$.

**NMR Spectroscopy.** NMR experiments were performed on a Bruker DRX 600 instrument, operating at 600 MHz for $^1$H NMR spectroscopy. 1D $^1$H NMR spectra were collected with a total of 32 K complex points and 64 transients. For all 1D and 2D spectra, the spectral width was 7200 Hz and a relaxation delay of 2 s was applied. The presaturation pulse sequence was used for the samples in $D_2O$ and double-pulsed field gradient spin−echo (dpfgsew5) pulse sequence was used for water suppression in $H_2O$ samples.[23] In the ROESY and NOESY experiments, a total of 2048 complex points in $t_2$ were typically collected for each of 256 $t_1$ increments, and 80−128 transients were averaged for each increment.

Two-dimensional [$^1$H, $^{15}$N] HMQC (heteronuclear multiple quantum coherence) spectra were recorded on the sample of $^{15}$N enriched *trans-EE* and its dinucleotide adducts.[24] The samples were prepared by dissolving the dinucleotides in 20 mM phosphate buffer (+10% $D_2O$, pH 6.5) and adding the *trans-EE* solution to make a 1:1 molar ratio. Since variation in pH during the reaction influences the exchange rate of the N−H protons and consequently affects the N−H cross-peak intensities, it was decided to use a phosphate buffer to ensure constant pH of 6.5. This condition is more biologically relevant, but at this pH a certain amount of *trans-EE* hydoxo species is formed in solution. Another complication encountered in performing this experiment was that the phosphate buffer is a potential ligand for platinum, and this has to be taken into account in the kinetic analysis. Typical acquisition parameters for two-dimensional [$^1$H, $^{15}$N] HMQC spectra were the following: In the first stage of the reaction, four transients were accumulated for each time point (gradually increased to 128 transients), 2 k complex points along $t_2$ and 32 along $t_1$, spectral width 6010 Hz for $^1$H and 1216 Hz for $^{15}$N. The experiment was optimized for one-bond $1J_{HN}$ = 78 Hz. The FIDs were multiplied by a square-cosine function and zero-filled to 2048 complex points along $t_1$ and $t_2$. The one-dimensional $^1$H FIDs were multiplied by an exponential window function prior to Fourier transformation. Typically, 0.3 Hz was added to the line widths. $^1$H spectra were referenced to the HDO-resonance set at 4.76 ppm and $^{15}$N spectra referenced to 1M $^{15}$N enriched $NH_4Cl$ in 1M HCl solution set at 0 ppm at 298 K.

Natural abundance [$^1$H, $^{15}$N] HMBC (heteronuclear multiple bond correlation) spectra were acquired for the HPLC fraction M2 of the *trans-EE*/r(ApG) reaction. The experiments were optimized for two-bond $^1$H−$^{15}$N connectivity involving nonexchangeable protons, where $\Delta = {}^1/_2 JNH = 48$ ms. Coupling constants $2J_{NH}$ for guanosine and adenosine were in the range 8−17 Hz. The $^1$H and $^{15}$N spectral widths were 2650 and 11950 Hz, respectively. The data were acquired

(15) Jamieson, E. R.; Lippard, S. J. *Chem. Rev.* **1999**, *99*, 2467−2498.
(16) Liu, Y.; Intini, F. P.; Natile, G.; Sletten, E. *J. Chem. Soc., Dalton Trans.* (in press).
(17) Liu, Y.; Pacifico, C.; Natile, G.; Sletten, E. *Angew. Chem. Int. Ed.* **2001**, *40*, 1226−1228.
(18) Warpehoski, M. A.; Harper, D. E. *J. Am. Chem. Soc.* **1995**, *117*, 2951−2952.
(19) Bevers, S.; Xiang, G.; McLaughlin, L. W. *Biochemistry* **1996**, *35*, 6483−6490.
(20) Sherman, S. E.; Lippard, S. J. *Chem. Rev.* **1987**, *87*, 1153−1181.
(21) Cini, R.; Caputo, P.; Intini, F. P.; Natile, G. *Inorg. Chem.* **1995**, *34*, 1130−1137.
(22) Liu, Y.; Sivo, M. F.; Natile, G.; Sletten, E. *Metal-Based Drugs* **2000**, *7*, 169−176.
(23) Liu, M.; Mao, X.; Ye, C.; Huang, H.; Nicholson, J. K.; Lindon, J. C. *J. Magn. Reson.* **1998**, *132*, 125−129. Hwang, T.-L.; Shaka, A. J. *J. Magn. Reson., Ser. A* **1995**, *112*, 275.
(24) Palmer, A. G.; Cavanagh, J.; Wright, P. E.; Rance, M. *J. Magn. Reson.* **1991**, *93*, 151. Kay, L. E.; Keifer, P.; Saarinen, T. *J. Am. Chem. Soc.* **1992**, *114*, 10663−10665. Schleucher, J.; Schwendinger, M.; Sattler, M.; Schmidt, P.; Schedletzky, O.; Glaser, S. J.; Sorensen, O. W.; Griesinger, C. *J. Biomol. NMR* **1994**, *4*, 301−306.

into 1024 complex points along $t_2$, 512 transients were averaged for 128 $t_1$ values, the recycling delay was 2 s, and the experimental time was 40 h.

**pH Measurements.** pH Measurements were made using a Philips PW 9420 pH meter equipped with a Sentron Red-Line semiconductor ion sensitive sensor calibrated with appropriate buffers. Values of pH were adjusted with $HClO_4$ or NaOH. This method of measuring pH instead of using a conventional glass electrode prevents contamination of the sample with chloride ions. The p$K_a$ values for the hydrolysis of *trans-EE* were obtained by pH titration using [$^1$H, $^{15}$N] HMQC spectroscopy to monitor the N−H signal. The pH titration curves for the signals of the dichloro and the solvated complexes are plotted in Figure S1. The p$K_a$ value estimate at ca. 5.8 for the deprotonation of the monochloro/monoaqua species is close to the corresponding value for cisplatin.[25] The p$K_a$ for deprotonation of the diaqua species of *trans-EE* could not be determined accurately because of overlapping with the region for deprotonation of the imino groups (ca. pH 8).

**Kinetic Measurements.** The HPLC fractions at different time points were normalized to the starting concentration of dinucleotide. For the $^{15}$N NMR data, the concentrations of each species were measured from the 2D N−H cross-peaks which were then normalized to the 1D proton spectra by comparing the aromatic signals of the dinucleotides with the methyl signals of *trans-EE*. The concentration of the dinucleotide was determined by UV. The concentrations of all species were evaluated at each time point and used as input data for the kinetic analysis. The appropriate differential equations were integrated numerically, and the rate constants were determined by a nonlinear optimization procedure using the program SCIENTIST (version 2.01, MicroMath Inc). In the kinetic analysis of the HPLC data, we used the hydrolysis constants for *trans-EE* previously determined by NMR. The errors given for the calculated rate constants represent one standard deviation.

**Molecular Modeling.** A model of the *trans-EE*/r(ApG) chelate was obtained by energy minimization and molecular dynamics calculations (BIOSYM) using distance constraints extracted from ROESY NMR spectra. The *trans-EE* ligands were initially fixed in the conformation as determined by X-ray structure analysis.[21] In the final calculation, only the platinum and the four nitrogen atoms were fixed in a square-planar arrangement.

## Results and Discussion

The kinetics study was performed by HPLC (reaction time of ca. 25 days). A typical HPLC profile, taken 48 h after mixing *trans-EE* and d(ApG), is shown in Figure 1a. The *trans-EE* platination reactions for d(ApG), d(GpA), and r(ApG) were monitored for 25 days and the species distributions versus time, as determined by HPLC, are plotted in Figure 2a−c. The reactions were carried out in acidic solution, and the pH (ca. 4) changed only slightly during the reaction. For d(GpA), the reaction was also carried out at an initial pH of 6.2 which dropped to 5.4 by the end of the reaction. In the latter case, the reaction rate decreased significantly as the pH was raised, that is, $t_{1/2}$ = 10.7 and 2.9 h for pH 6.2 and 4.0, respectively.

At each time point, aliquots were collected and immediately loaded on the HPLC column. Since each HPLC experiment takes 30−50 min, the initial stage of the reactions is not well defined. A common procedure used to alleviate this problem is to add large amounts of KCl or KBr, as quenching agents to arrest the reaction, before carrying out the HPLC analysis. However, this method may lead to significant removal of platinum from the platinated nucleotide before the HPLC analysis is completed and may introduce an extra source of error.

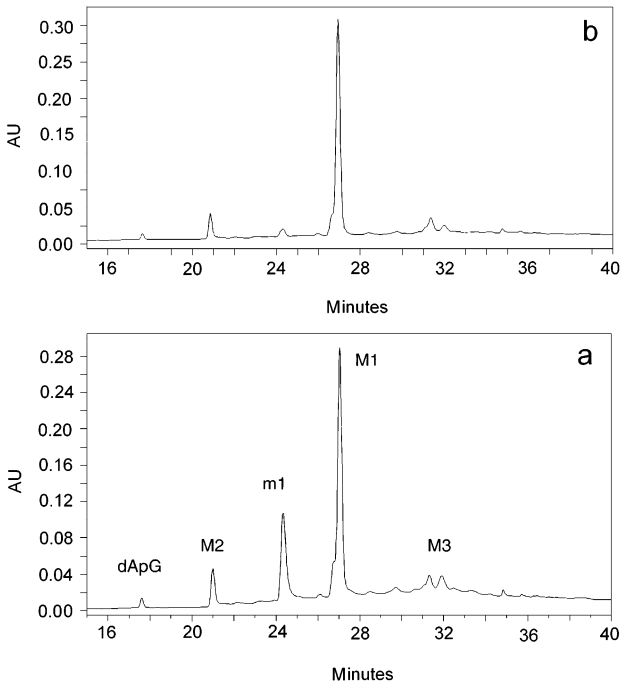


***Figure 1.*** Typical HLPC profiles. (a) Reaction between *trans-EE* and d(ApG) 48 h after mixing of the reactants. (b) Conversion of m1 to M1 by addition of 1M NaCl.

Murdoch et al.[26] have reported that in the sample of a platinated oligonucleotide containing 3 M KCl, ca. 40% of the platinated species had been converted to free DNA after 6 days. Being a noninvasive direct method $^{15}$N NMR spectroscopy could, in principle, allow more reliable kinetic determinations than HPLC. However, for very slow reactions (weeks), the HPLC method is usually more convenient.

In each experiment depicted in Figure 2a−c, the amount of G−N7/monochloro adduct (M1) reaches a maximum after about 10 h. The minor product m1 represents the G−N7/monoaqua adduct and was identified by addition of 1M NaCl which represses the concentration of m1 in favor of M1 (Figure 1b). A similar behavior was also observed in the reaction of *trans-EE* with GMP.[22] The reaction rates expressed by the half-life ($t_{1/2}$) of the free dinucleotides are r(ApG) 1.6 h, d(ApG) 2.3 h, and d(GpA) 2.9 h. For r(ApG) and d(ApG), the M1 adduct undergoes a slow trans-chelation reaction forming a bifunctional (A−N3, G−N7) chelate (M2) which was isolated and characterized by NMR (see below). In contrast, for d(GpA) the M1 adduct is not converted to a bifunctional chelate. HPLC analysis of the d(GpA) reaction mixture, recorded after two weeks, displayed only the M1 and m1 peaks (Figure S2). Also at acidic pH, d(GpA) does not form M2 chelates (Figure S3). Evidently, the chelate formation is favorable for ApG but not for GpA.

The proposed reaction mechanism is shown in Scheme 1 and the rate constants for each reaction step are listed in Table 1. Expanding Scheme 1 by taking into account the direct substitution pathways A → M1 and M1 → M2 gave rate constants for these steps 2 orders of magnitude smaller than those for the steps via solvato species. In the fitting of the experimental data, these steps were left out. As expected, the $k_3$ values for the formation of *trans-EE* G−N7/monochloro adducts determined

(25) Berners-Price, S. J.; Frenkiel, T. A.; Frey, U.; Ranford, J. D.; Sadler, P. J. *J. Chem. Soc., Chem. Commun.* **1992**, 789−791.

(26) Murdoch, P. del S.; Guo, Z.; Parkinson, J. A.; Sadler, P. J. *J. Biol. Inorg. Chem.* **1999**, *4*, 32−38.

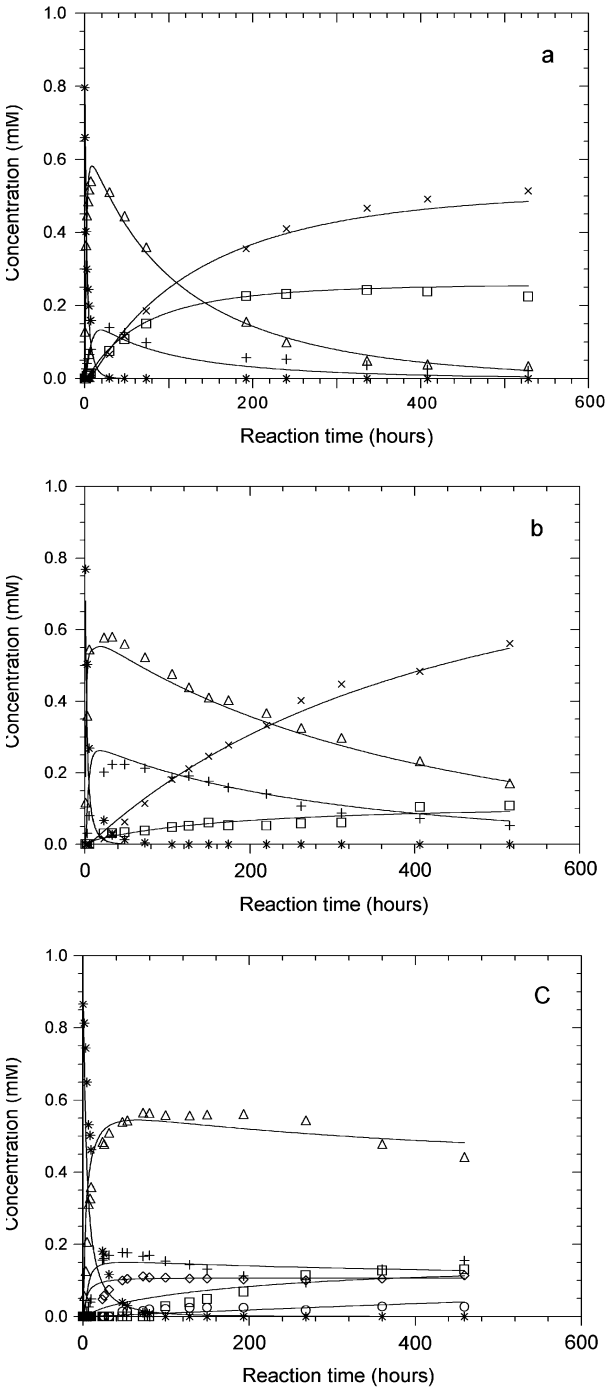


***Figure 2.*** Experimental concentrations (HPLC data) and theoretically fitted curves for the reaction of 1 mM *trans-EE* with (a) 0.8 mM r(ApG), (b) 0.9 mM d(ApG), and (c) 0.9 mM d(GpA). Symbols: (*) free nucleotides, (△) M1, (+) m1, (×) M2, (□) M3; for (c) also (◇) m2, (○) m3.

at acidic pH (4.0) are larger than the value determined for d(GpA) at higher pH (6.2), indicating that at higher pH most of the monoaqua species is transformed into the monohydroxo species. The experimental data for the hydrolysis of the M1 species ($k_4$ and $k_{-4}$) could not be fitted properly in d(GpA) (fairly large standard deviation) since for this latter sequence there is no formation of A−N3/G−N7 chelate and two additional species (m2 and m3) are formed after several weeks of reaction time. These species are tentatively included in the fitting procedure as mono adducts of adenine. The reaction rate for formation of M2 is faster in r(ApG) ($k_5 = 5.1 \times 10^{-6}$) than in d(ApG) ($k_5 = 2.1 \times 10^{-6}$). The same difference can be observed also for the half-life of M1 which is longer for the d(ApG) adduct ($t_{1/2} = 297$ h) than for the r(ApG) adduct ($t_{1/2} = 101$ h).

**Kinetics Study Performed by [$^1$H, $^{15}$N] HMQC NMR (Reaction Time of ca. 1 Day).** The reactions between *trans-EE* and the dinucleotides r(ApG), d(ApG), and d(GpA) were also monitored by recording [$^1$H, $^{15}$N] HMQC spectra at different time intervals. In the early stage of the reactions, spectra with sufficient S/N were recorded every 5 min. Typical HMQC spectra for the reaction between *trans-EE* and r(ApG) are shown in Figure 3. The assignment of the cross-peaks was carried out by comparison with previously recorded spectra for the reaction between *trans-EE* and GMP.[16] After 45 min (Figure 3a), the strong cross-peaks (A) at 7.42/86.93 ppm and (B) at 7.51/90.29 ppm represent *trans-EE* dichloro and *trans-EE* monochloro/monoaqua species, respectively. Peaks at 7.79/89.51 and 7.96/93.83 ppm are assigned to the *trans-EE* G−N7/monochloro (M1) and *trans-EE* G−N7/monoaqua (m1) adducts, respectively. The major peak (P) at 7.59/90.56 ppm is assigned to the *trans-EE* monochloro/monophosphate species. The degree of involvement of the phosphate buffer in binding to Pt-complexes has often been a subject of controversy.[27] However, our assignment of the N−H proton representing the Pt−$PO_4$ adduct is confirmed by comparison with the [$^1$H, $^{15}$N] HMQC spectra obtained in the reaction of *trans-EE*/GMP either in the presence or in the absence of 20 mM phosphate buffer.[16] Additional evidence in support of the given assignment was obtained by recording the $^{31}$P NMR spectrum (Figure S4) which indicates that a platinum phosphate adduct is formed in solution of *trans-EE* in phosphate buffer. In the HMQC spectrum recorded after 6 h (Figure 3b), the new peak (m1) at 7.96/93.83 ppm is assigned to the monoadduct having a water molecule trans to the coordinated G−N7. In the HMQC spectrum recorded after 28 h (Figure 3c), one prominent new peak (Q) at 7.86/93.53 ppm was assigned to the monoadduct having a phosphate trans to the coordinated G−N7. A HMQC spectrum recorded after 18 days (data not shown) contains other cross-peaks representing minor adducts which were not characterized.

The peak intensities versus time for the main products produced during the first 20 h of the *trans-EE*/r(ApG) reaction are plotted in Figure 4. Similar reaction profiles for *trans-EE*/(ApG) and *trans-EE*/(GpA) are reported in Figure S5. Kinetic fits to the reaction profiles were carried out according to the first part of Scheme 1, and the rate constants for each reaction step are listed in Table 2. The rate constants $k_1$ and $k_{-1}$ for the hydrolysis of *trans-EE* are reasonably close to those published earlier for reaction of *trans-EE* with GMP.[16] The rate constants for the reactions between *trans-EE* monochloro/monoaqua and the dinucleotides ($k_3$) were almost 1 order of magnitude lower than those determined by HPLC (Table 1) except for $k_3$ of d(GpA) which was measured at neutral pH.

The discrepancy between the rate constants obtained by HPLC and those obtained by $^{15}$N NMR spectroscopy is a consequence of the different pH used in the two sets of experiments. For the reactions in acidic solution (monitored by HPLC), the *trans-EE* monochloro/monoaqua complex is the dominant solvato species in solution, while in the reactions at neutral pH (monitored by [$^1$H, $^{15}$N] HMQC NMR), the dominant solvato

(27) Legendre, F.; Veronique, B.; Kozelka, J.; Chottard, J.-C. *Chem. Eur. J.* **2000**, *6*, 2002−2010.

***Scheme 1.*** Proposed Mechanism for Reaction of *trans-EE* with r(ApG) or d(ApG)

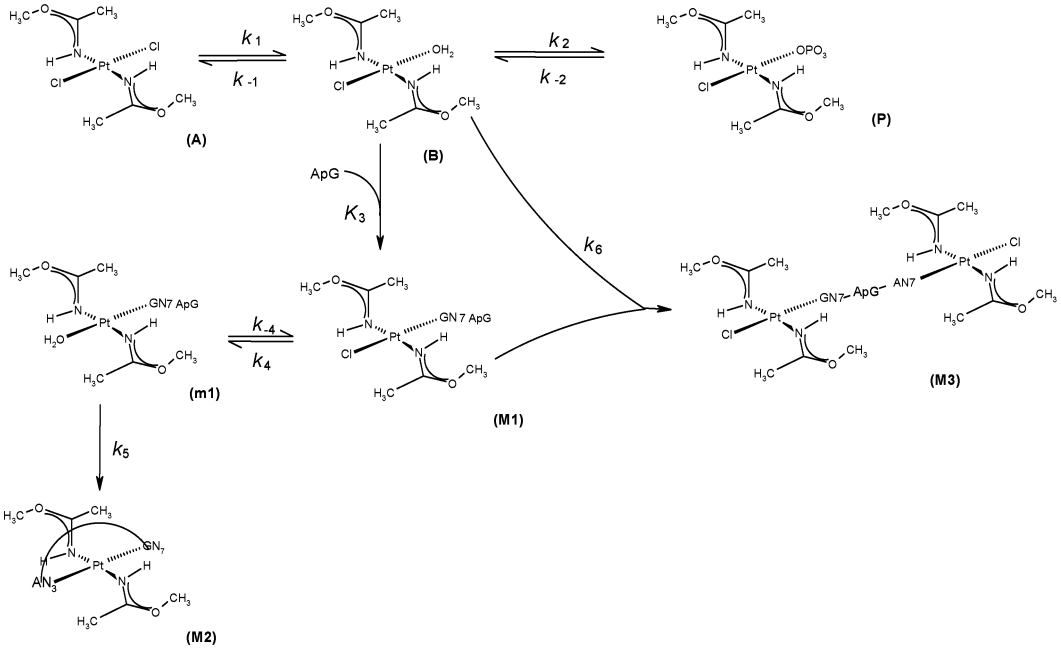


***Table 1.*** Optimized Rate Constants (Standard Deviations in Parentheses) for Platination of Dinucleotides (**1**−**3**) with *trans-EE* at 298 K and pH = 4.0 ± 0.2 (1and 2) and 6.2−5.4 (3). The Reactions Were Monitored by HPLC

| | | $k_3$ ($s^{-1}$•$M^{-1}$) | $k_4$ ($s^{-1}$) | $k_4$ ($s^{-1}$•$M^{-1}$) | $k_5$ ($s^{-1}$) | $k_6$ ($s^{-1}$•$M^{-1}$) |
|---|---|---|---|---|---|---|
| **1** | r(ApG)[a] | 0.33(2) | $2.6(6) \times 10^{-5}$ | 0.064(20) | $5.1(6) \times 10^{-6}$ | 0.014(2) |
| **2** | d(ApG)[a] | 0.38(3) | $3.9(9) \times 10^{-5}$ | 0.064(16) | $2.1(1) \times 10^{-6}$ | 0.0091(7) |
| **3** | d(GpA)[b] | 0.095(7) | $3.1(19) \times 10^{-5}$ | 0.099(66) | | 0.0030(7) |

[a] pH = 4.0 ± 0.2. [b] pH between 5.4 and 6.2.

species is the monochloro/monohydroxo complex. The latter species is expected to be much less reactive toward nucleotides than the corresponding monoaqua complex.[27] In conclusion, both HPLC and NMR experiments indicate that there is no significant difference between ApG and GpA for monofunctional binding to *trans-EE*.

**Characterization of Isolated Monofunctional Adducts M1.** The $^1$H chemical shifts of the M1 HPLC fractions are listed in Table S1. Downfield shifts of the G−H8 resonances in the range of 0.48−0.60 ppm are in accord with G−N7 platination. Other resonances show only minor shifts (0.1−0.2 ppm). The assignments were based on 2D COSY and ROESY spectra. $T_1$ measurements gave additional support for distinguishing between A−H2 (long $T_1$) and A−H8 (short $T_1$) signals. Figure S6 shows the ROESY spectra for the M1 adducts of r(ApG) and d(ApG). In each spectrum, cross-peaks between the methyl and methoxy groups of *trans-EE* and the sugar/base protons of the guanine and adenine residues are observed. The chemical shifts of free r(ApG) and d(ApG) nucleotides are in accord with those published by van Hemelryck.[28]

The cross-peaks in the 2D $^1$H NMR spectra were integrated and the intensities converted to distances using the usual $r^{-6}$ distance dependence and a H5′/H5″ distance of 1.8 Å as a measuring stick. The calculated distances were based on only one set of ROESY peaks; thus, the distance constraints obtained were not very reliable.

**Characterization of Isolated trans-Chelate Bifunctional Adducts M2.** The 2D $^1$H ROESY spectrum of the M2 HPLC fraction of *trans-EE*/r(ApG) and the 1D $^1$H NMR spectrum of free r(ApG) are shown in Figure 5.

One may notice two unusual features of the spectra related to the adenosine residue: (i) an extreme downfield chemical shift ($\Delta\delta$ = 3.68 ppm) for the anomeric proton A−H1′ and (ii) a relatively large downfield chemical shift ($\Delta\delta$ = 0.82 ppm) for the aromatic proton A−H2. In addition, most of the other sugar protons on the adenosine residue exhibit significant downfield shifts. The assignments of adenine H2 versus H8 were confirmed by measuring $T_1$ relaxation times: A−H2 (4.2 s), A−H8 (1.9 s), G−H8 (2.2 s). The cross-peak AH1′/AH2′ in the COSY NMR spectrum provides additional evidence for the assignment of AH1′.

To explain the unusual chemical shift pattern for the adenosine resonances, one has to invoke a completely new model for the platinum coordination to the purine dinucleotide. For stereochemical reasons, *trans*-Pt compounds are unable to cross-link the two purines in r(ApG) through A−N7/G−N7 or A−N1/G−N7 coordination. Consequently, if G−N7 is one of the binding sites, the second binding site must be A−N3. This model can account for both the large downfield shift of A−H2 and the normal (for a N7 coordinated G) downfield shift of G−H8.

**$^{15}$N Natural Abundance NMR.** An elegant method for proving the A−N3/G−N7 coordination of the dinucleotide was based on $^1$H-detected [$^1$H, $^{15}$N] HMBC (heteronuclear multiple bond correlation) spectroscopy. This technique is characterized by a very high sensitivity and can be applied to samples with natural abundance $^{15}$N.[29,30] The 2D HMBC spectra recorded for free r(ApG) and its M2 fraction is shown in Figure 6 a and b. The $^{15}$N resonances of G−N7 and A−N3 are shifted upfield by 99 and 83 ppm, respectively, while the other nitrogen atoms exhibit only minor downfield shifts. These results prove

(28) van Hemelryck, B.; Girault, J.-P.; Chottard, G.; Valdon, P.; Laoui, A.; Chottard, J.-C. *Inorg. Chem.* **1987**, *26*, 787−795.
(29) Bax, A.; Summers, M. F. *J. Am. Chem. Soc.* **1986**, *108*, 2093−2094.
(30) Chen, Y.; Guo, Z.; Sadler, P. J. In *Cisplatin. Chemistry and Biochemistry of a Leading Anticancer Drug*; Lippert, B., Ed.; Wiley-VCH: Zurich, 1999; pp 293−318.

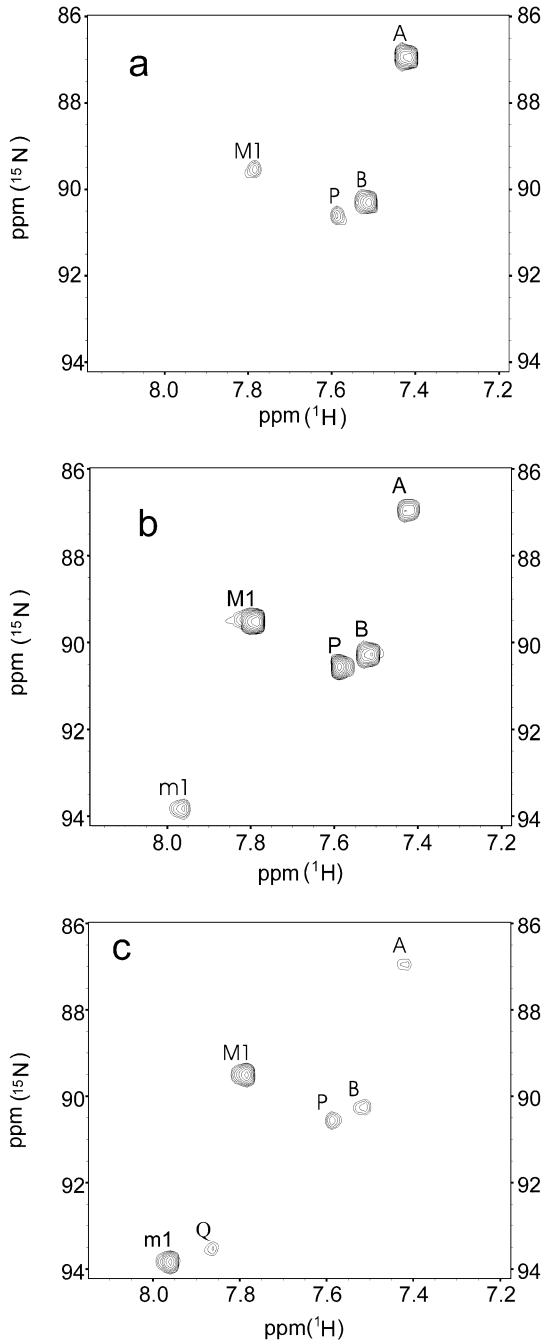


***Figure 3.*** [$^1$H, $^{15}$N] HMQC spectra of a 1 mM solution of *trans-EE*/r(ApG) (1:1), 20 mM phosphate buffer and 10% $D_2O$, recorded after 45 min (a), 6 h (b), and 28 h (c).

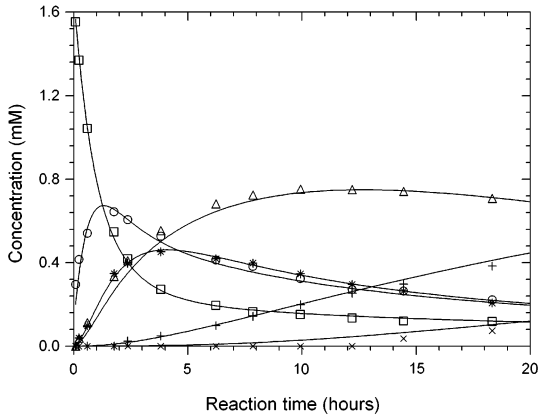


***Figure 4.*** Experimental concentrations (NMR data) and theoretically fitted curves for the reaction between 0.8 mM *trans-EE* and 0.9 mM r(ApG) in 20 mM phosphate buffer. Symbols: (□) *trans-EE*; (○) *trans-EE* monoaqua/monochloro; (△) M1; (+) m1; (*) *trans-EE* monochloro/monophosphate; (×) *trans-EE* G−N7/monophosphate.

***Table 2.*** Optimized Rate Constants (Standard Deviations in Parentheses) for the First Stage (ca. 1 Day Reaction Time) of the Reaction between *trans-EE* and Dinucleotides **1**−**3** Performed at 298 K and pH 6.5 (20 mM Phosphate Buffer)[a]

| | | $k_1$($s^{-1}$) ($\times10^{-4}$) | $k_{-1}$ ($M^{-1}$ $s^{-1}$) | $k_2$($s^{-1}$) ($\times10^{-4}$) | $k_{-2}$($s^{-1}$) ($\times10^{-4}$) | $k_3$ ($M^{-1}$ $s^{-1}$) | $k_4$($s^{-1}$) ($\times10^{-6}$) | $k_{-4}$ ($M^{-1}$ $s^{-1}$) ($\times10^{-3}$) |
|---|---|---|---|---|---|---|---|---|
| **1** | r(ApG) | 2.00(7) | 0.096(9) | 1.2(1) | 1.3(1) | 0.091(1) | 1.19(6) | 1.6 (8) |
| **2** | d(ApG) | 2.72(8) | 0.119(9) | 1.6(1) | 1.7(1) | 0.056(1) | 1.2(1) | 1(2) |
| **3** | d(GpA) | 2.59(5) | 0.090(8) | 1.6(2) | 1.5(1) | 0.063(2) | 1.4(8) | 1(1) |

[a] The reactions were monitored by [$^1$H, $^{15}$N] HMQC NMR spectroscopy.

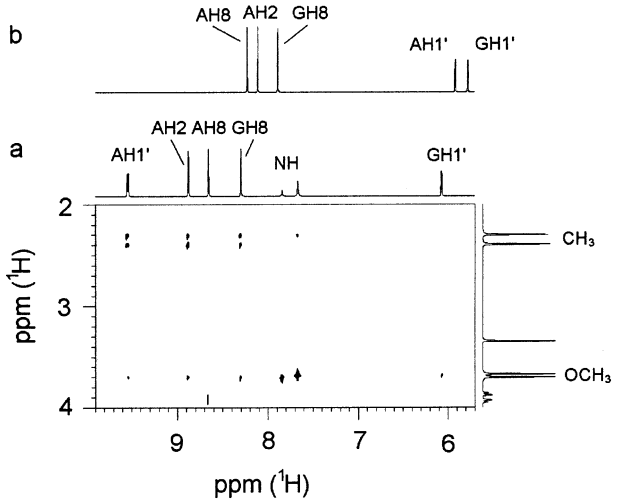


***Figure 5.*** $^1$H NMR 1D and 2D spectra of *trans-EE*/r(ApG) bifunctional adduct M2 (a), and 1D spectrum of free r(ApG) (b).

conclusively that A−N3 is indeed involved in coordination to platinum. Adenine N3 is the least basic site of the ring nitrogen atoms of adenine and only a few examples are known where metal ions bind to A−N3.[31−33]

**Dependence of Chemical Shifts upon pH.** The differences in coordination mode between monofunctional M1 and bifunctional M2 adducts are clearly evident also from plots of chemical shifts versus pH. The pH titration curves for the M1 and M2 adducts formed in the reaction of *trans-EE* with r(ApG) are shown in Figure 7. Similar plots for d(ApG) and d(GpA) are reported in Figure S7 of Supporting Information.

The pH dependence of G−H8 chemical shifts confirms platination at G−N7 in both adducts. The M1 protonation of A−N1 (apparent p$K_a$ ∼ 3) causes a large change in chemical shift of both A−H2 and A−H8 and, to a smaller extent, also of G−H8. The situation is quite different for the adenine protons of the trans-chelate M2. The invariance of the H2/H8 shifts may indicate either platination at N1 or, alternatively, platination at N3. The latter platination would produce a p$K_a$ shift of A−N1 below the range of pH explored. In support of the latter

(31) Meiser, C.; Song, B.; Freisinger, E.; Peilert, M.; Sigel, H.; Lippert, B. *Chem. Eur. J.* **1997**, *3*, 388−398.
(32) Price, C.; Shipman, M. A.; Rees, N. H.; Elsegood, M. R. J.; Edwards, A. J.; Clegg, W.; Houlton, A. *Chem. Eur. J.* **2001**, *7*, 1194−1201.
(33) Blindauer, C. A.; Emwas, A. H.; Holy, A.; Dvorakova, H.; Sletten, E.; Sigel, H. *Chem. Eur. J.* **1997**, *3*, 1526−1536.

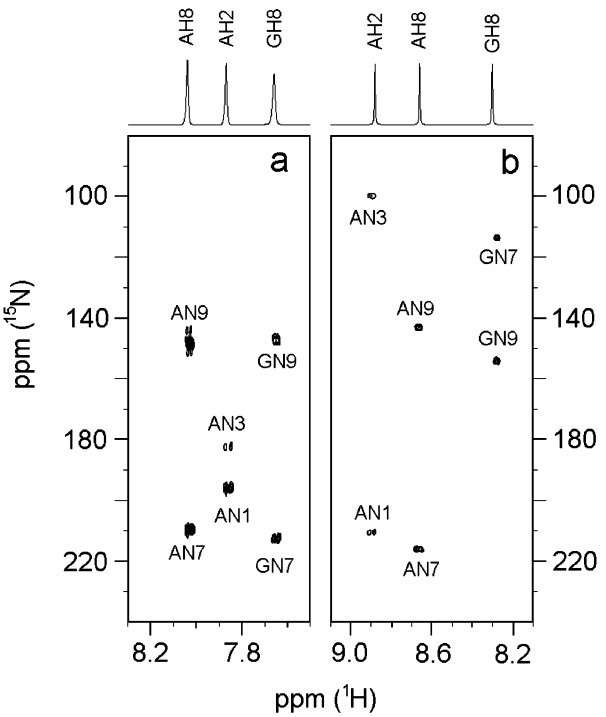


***Figure 6.*** [$^1$H, $^{15}$N] HMBC NMR spectra. (a) free r(ApG), (b) *trans-EE*/r(ApG) adduct M2.

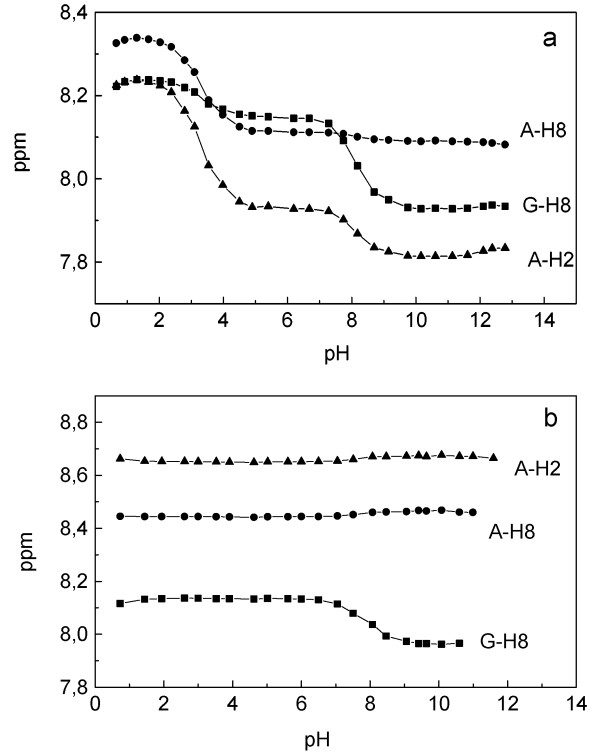


***Figure 7.*** $^1$H NMR chemical shifts vs pH for A−H8, G−H8, and A−H2 in the *trans-EE*/r(ApG) adducts M1 (a) and M2 (b).

hypothesis are the reported estimates of p$K_a$ values for N1 and N7, in N3-platinated N6,N6,N9-trimethyladenine, of −1.2 and 0.3, respectively.[31]

**Molecular Modeling.** The distance constraints obtained from the ROESY spectra of the r(ApG) M2 adduct were used, with relatively wide margins for upper and lower distance limits, as input data for the molecular modeling program BIOSYM.[34] The

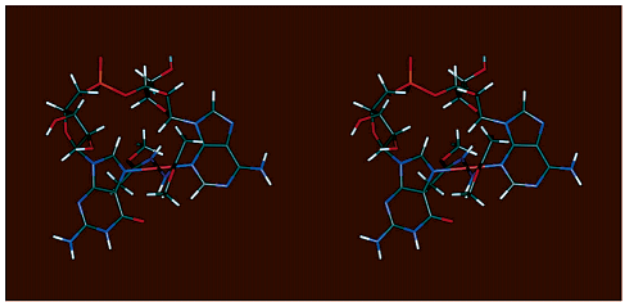

***Figure 8.*** Stereoview of the molecular model of the *trans-EE*/r(ApG) (N3, N7) adduct M2.

model was optimized by energy-minimization calculations using constraints for contacts between *trans-EE* methyl/methoxy groups and nucleotide protons. The *trans-EE* ligands were initially fixed in the conformation determined by an X-ray structure analysis.[21] In the final calculation, only the platinum and the four nitrogen atoms were fixed in a square-planar arrangement. The molecular model obtained by the minimization process is presented as a stereopair in Figure 8. The results are in qualitative agreement with the experimental data.

One important aspect of the model is the location of the anomeric proton A−H1′ close to the platinum center (2.29 Å). This may explain the very large ($\Delta\delta$ = 3.68 ppm) downfield shift resulting from the paramagnetic anisotropy of platinum. It has been shown that protons located at a pseudoaxial position above a platinum center in square-planar complexes may experience large downfield shifts. In the crystal structure of *trans*-[$PtCl_2$(benzoquinoline)($PEt_3$)], a Pt···H distance of 2.53 Å was found for a benzoquinoline proton, and in solution this proton experienced a downfield shift of 2.75 ppm.[35] Therefore, the large downfield shift of A−H1′ is in accord with the A−H1′···Pt distance of 2.29 Å suggested by our model. Similar results were observed in the *trans-EE*/d(ApG) adduct M2 for which the AH1′ signal (9.80 ppm) was shifted downfield by 3.64 ppm.

Another important feature of the proposed model is the close contact between the 2′ oxygen of the adenine ribose and platinum. This may help in stabilizing the chelate geometry and could probably explain why r(ApG) forms the M2 chelate adduct at a faster rate than d(ApG). d(GpA), on the other hand, does not form a chelate even after two weeks of reaction. In all cases, the first step in the reaction with *trans-EE* is likely to be N7-coordination of the guanine residue. For d(ApG) and r(ApG), the coordinated guanine will have the adenine residue in 5′-position. A 5′ residue is usually able to reach over the coordinated metal moiety and to interact with it (this is the case of the 5′-phosphate of a coordinated 5′-GMP which is able to interact with a cis amine). In the case under investigation, the two cis positions are kept by iminoether ligands; therefore, the only chance for the adenine to interact with platinum is to reach over the trans position and displace the coordinated water molecule. Such a rearrangement is very rare in platinum chemistry since it requires the closure of a very large chelate ring; however, it is not forbidden. Therefore, a cross-link spanning trans positions is formed by coordination of A−N3.

(34) *BIOSYM User Guide for InsightII* (version 2.3.5), Discover (version 2.9.5), and NMR Refine (version 2.3), 1993.
(35) Albinati, A.; Pregosin, P. S.; Wombacher, F. *Inorg. Chem.* **1990**, *29*, 1812−1817.

Coordination to platinum of A−N7 or A−N1 probably would require a more severe stretch of the sugar−phosphate backbone.

In the d(GpA), coordination to platinum of G−N7 places the adenine residue in 3′ position, away from the metal center and unable to give the trans-chelation reaction (the phosphate in 3′ position of a coordinated 5′-GMP is unable to interact with a cis amine).

**Characterization of Isolated Binuclear Adducts M3.** Another major adduct, M3, is formed if *trans-EE* is present in excess with respect to the dinucleotide r(ApG) (Figure 1a). 1D $^1$H NMR spectra of this fraction are distinctly different from those obtained for M1 and M2. The integration of the 1D $^1$H spectra (Figure S8) indicates that the composition of M3 corresponds to a *trans-EE*/r(ApG) ratio of 2:1. It can be shown from ROESY spectra that the two sets of $CH_3/OCH_3$ signals at 3.75/2.46 and 3.72/2.40 ppm belong to *trans-EE* bound to adenine and guanine, respectively (see Table S2). The downfield chemical shifts of G−H8 ($\Delta\delta$ = 0.60 ppm) and A−H8 ($\Delta\delta$ = 0.82 ppm) indicate that both G−N7 and A−N7 are coordinated to platinum. The pH profiles of the aromatic protons are shown in Figure S9. The change in chemical shift of G−H8 gives a p$K_a \approx 8$ for G−N1 deprotonation and is in accord with platination at G−N7. Change in chemical shifts of A−H2 and A−H8 protons gives a p$K_a \approx 1$ for A−N1 in accord with platination at N7 (p$K_a$ of 3.5 for free r(ApG)).

**Reaction of *trans*-DDP with d(ApG).** The A−N3/G−N7 chelation of adjacent purines observed in the reaction of *trans-EE* with d(ApG) and r(ApG) has never been reported for *trans*-DDP reactions with di- or oligonucleotides. Stereochemically, *trans*-DDP should have the same ability as *trans-EE* to form an A−N3/G−N7 chelate. However, since the chelate formation is quite slow, it may not have been recognized yet. The reaction between *trans*-DDP and d(ApG) was monitored both by HPLC and $^1$H NMR. The HPLC curves recorded over several hours of reaction time (Figure 9) show that *trans*-DDP produces many more adducts than *trans-EE*. Only the first major adduct was separated by HPLC and characterized by NMR. This adduct is similar to the *trans-EE*/d(ApG) M1 adduct with monofunctional platination at G−N7. Other adducts could not be separated in sufficient amounts to allow their characterization by NMR. The 1D $^1$H NMR spectrum of the reaction mixture shows several overlapping resonances; however, after two weeks of reaction time, an A−H1′ signal is well visible in about the same extreme low-field position as the A−H1′ signal of the M2 compound formed in the reaction of *trans-EE* with d(ApG). The initial rate for reaction of *trans*-DDP with d(ApG), as expressed by the d(ApG) half-life ($t_{1/2}$ = 3 h), is not significantly different from that found in *trans-EE* ($t_{1/2}$ = 2.3 h). However, the half-life of the *trans*-DDP/d(ApG) M1 adduct ($t_{1/2}$ = 56 h) is shorter than those of *trans-EE*/d(ApG) and *trans-EE*/r(ApG) M1 adducts ($t_{1/2}$ = 297 and 101 h, respectively). Thus, the steric effect imposed by the bulky iminoether ligands does not influence significantly the reaction rate for formation of the monofunctional adducts but, instead, significantly influences the subsequent M1 → M2 reaction.

In conclusion, both HPLC and $^1$H NMR data indicate that also *trans*-DDP, like *trans-EE*, is able to form M2 chelates, and formation of cross-links spanning trans-positions appears to be an intrinsic property of trans-platinum complexes.

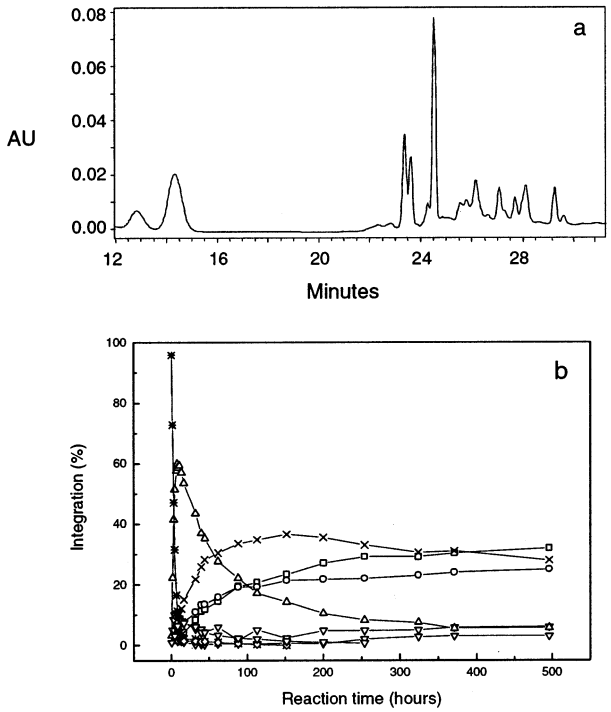


***Figure 9.*** HPLC traces for the reaction of *trans*-DDP with d(ApG); (a) after 371 h; (b) species distribution as a function of reaction time. Tentative assignment of the HPLC peaks representing different adducts of *trans*-DDP: (*) d(ApG); (△) M1; (×), (□), and (○) were not assigned, but one of them most likely represents the bifunctional chelate M2.

## Conclusions

This investigation has demonstrated, beyond any reasonable doubt, that trans-oriented platinum complexes are capable of forming 1,2-bifunctional adducts with single-strand oligonucleotides. So far, formation of such a cross-link spanning two trans positions has been observed only in the ApG sequence and involves coordination to platinum of adenine N3 and guanine N7. Other possible coordination modes such as A−N7/G−N8 and A−N1/C−N7 probably would require a much more severe stretch of the dinucleotide frame.

The first step in the reaction is coordination to platinum of guanine N7 followed by a very slow trans-chelation reaction. The latter reaction is very rare in platinum chemistry (usually chelation occurs in cis positions) probably because it requires formation of a very large ring. A distinct feature of this cross-link spanning two trans-positions is a very large downfield shift of the A−H1′ proton (3.68 ppm); molecular models indicate that this proton sits on the platinum atom at a distance of 2.29 Å. The presence of this unique A−H1′ resonance in the reaction of *trans*-DDP with d(ApG) indicates that a similar adduct is formed also in the latter case. Therefore, formation of an A−N3/G−N7 1,2 trans-chelate is not a peculiar feature of trans-iminoether platinum substrates but is general for trans-oriented platinum substrates, although it might not be always the preferential reaction path.

An interesting observation was the total absence of trans-chelate 1,2-cross-link formation in the reaction with the reverse GpA sequence. This finding has been correlated with the inability of the adenine in 3′ position of the G−N7 coordinated monofunctional Pt/r(GpA) adduct to reach over the platinum center and to interact with it. Of course, the situation is very different for an adenine in 5′ position of a G−N7 coordinated

Pt/(ApG) monofunctional adduct. This finding has an astonishing similarity with the adenine/guanine 1,2-intrastrand cross-link formed in the reaction of *cisplatin* with DNA. Also in this case, it is required that the adenine is in 5′ position with respect to the guanine base.

Another noteworthy observation was the faster rate of formation of the trans-oriented cross-link in the r(ApG) system with respect to the d(ApG) context. In the proposed model, a close contact between the 2′ oxygen of the adenine ribose and the platinum center has been found. This result may indicate that the A−N3/ G−N7 trans-chelate could play an important role in the interaction of trans-oriented platinum substrates with RNA sequences rather than with DNA.

Finally, a distinct feature of the ribo-dinucleotides, with respect to the deoxyribo sequence, was observed also in the formation of the dinuclear adducts Pt-ApG-Pt. The coordination was exclusively at A−N7/G−N7 in the former case while in the latter case both A−N7/G−N7 and A−N1/G−N7 adducts were formed.

Taken together, the results of this work open new perspectives in the mode of interaction of trans-oriented platinum drugs with nucleic acids.

**Acknowledgment.** We thank the Norwegian Research Council (Contract 135055/432) and the Italian M.I.U.R. (Cofin. N. 2001053898) for financial support. We have also benefited from stimulating discussions with Dr. Jorma Arpalahti, University of Turku, and other working group members of the COST Action D20.

**Supporting Information Available:** Figures of $^{1}H$ and $^{15}N$ chemical shifts, HPLC profiles, $^{31}P$ NMR spectra, species distribution, and ROESY NMR spectra and tables of chemical shifts (PDF). This material is available free of charge via the Internet at http://pubs.acs.org.

JA027251N